Low-Noise High-Sensitivity Observation of Electromagnetic Precursors of Large Earthquakes in Japan

Masafumi Fujii[1]*

[1]Graduate Research Division of Science and Engineering, University of Toyama

Key Points:

- Detection of the electromagnetic precursors of earthquakes has been achieved by a high-sensitivity low-noise observation method of VHF radiowave
- A super-narrowband notch (band-rejection) filter reduces intermodulation noises significantly and makes earthquake precursors detectable
- Remarkable electromagnetic precursors are observed for the Fukushima offshore earthquake M7.4 on March 16, 2022

*3190 Gofuku Toyama, Japan

Corresponding author: Masafumi Fujii, mfujii@eng.u-toyama.ac.jp

Abstract

Detection of precursors of earthquakes has long been a controversial issue in regard to its possibility and realizability. Here we present successful and stable observation of the electromagnetic precursors of earthquakes in Japan using a specifically designed narrowband filter to suppress noises for a radiowave at the very high frequency (VHF) range. Electromagnetic precursors are observed consistently with our high-sensitivity low-noise equipment as sudden rises and/or falls of received radiowave power in a time scale of a few hours. The signals are distinctive from other electromagnetic noises and observed typically some hours to some days before large earthquakes. We have observed numerous precursory signals of earthquakes for several years. Recently, we obtained surprisingly clear precursory signals at two different locations more than 200 km apart a day before the Fukushima offshore, the Pacific side of Japan, M7.4 earthquake on March 16, 2022. We identified carefully the signals as precursors of the earthquake by comparing the signals in time with the meteorological, ionospheric, geomagnetic field data. Observation of such radiowave precursors contributes to the prediction of earthquakes as well as monitoring the lithospheric stress and pre-seismic activity over a broad area of a few hundred kilometers.

1 Introduction

Electromagnetic signals could be enhanced and received at distant locations some days or weeks before earthquakes. Researchers have tried to observe such electromagnetic anomalies and precursors associated with earthquakes for more than 20 years (Fujiwara et al., 2004; Moriya et al., 2005; Bakun et al., 2005; Hayakawa et al., 2007; Uyeda et al., 2009; Moriya et al., 2009, 2010; Kushida, 2012; Bleier et al., 2013). The observation of such anomalies has been difficult and unstable because they are affected by geographical, atmospheric, ionospheric conditions and disturbed by various environmental noises of a random nature.

On the other hand, the mechanism of the anomalous radiowave propagation has been explained reasonably by the theory of ground surface plasma waves appearing on the surface of the earth (Fujii, 2013, 2016). It has been experimentally shown that positive charge carriers come out from the peroxy bond in oxidized minerals when rocks are subjected to tectonic deviatoric stresses (Freund, 2000, 2002, 2011; Bleier et al., 2013). Although it is still controversial, this fact could explain the possibility of electrostatic charges on the earth's surface associated with co-seismic or pre-seismic activities. In general, if electrical charges exist on a surface, then the charges oscillate with the external electric field. This is equivalent to the well-known surface plasmon in optics induced by light on metal surfaces (Kittel, 1986; Raether, 1977, 1988; Fujii, 2014).

Here, we assume that a sufficient amount of charge carriers exist on the earth's surface, then an oscillation of the surface charge carriers is induced by a radiowave over the ground surface (Fujii, 2013, 2016), referred to as a terrestrial ground surface plasmon. The charge density has been estimated experimentally by applying a stress to a gabbro tile (Scoville et al., 2015), which shows that a sufficient amount of surface charge carriers are involved before earthquakes and the terrestrial ground surface plasmon can be induced. Such mobile charge carriers of the same sign diffuse by electrical repulsive forces. In mountainous regions, the charge carriers move to sharp wedges or peaks of mountains, then the vertically polarized electric field becomes dominant. In contrast, when the charge carriers appear near a coastline or in the ocean, they would not accumulate but diffuse to recombine with electrons and disappear; cliffs and/or beaches in a coastline may lead to a different appearance and polarization of the radiowave anomaly than in mountainous regions. Therefore,

it is important to consider the mechanism of the radiowave propagation even for the experimental observation of precursory signals of earthquakes.

This paper reports a highly sensitive low-noise observation technique of anomalous signals carried by VHF radiowaves. To detect the electromagnetic precursors that are subtle and nearly random, a notch filter, or a band-rejection filter, having a super-narrow bandwidth has been implemented in our observation systems. The filter reduces the noise level significantly and allows the detection of the precursory signals steadily and clearly.

In addition, the recent observation of the electromagnetic precursors with our system is presented, which are clear signals before large earthquakes. The observation has been performed both in Toyama city on the west side of Japan, and in Iwata city facing the Pacific Ocean, located on the opposite sides of the Japan Island. A large earthquake occurred at the Fukushima offshore of Pacific Ocean on March 16, 2022. Since some days before the event, we had detected large electromagnetic precursors in the radiowave signals. The measured precursory signals have been carefully compared with other possible noises generated by the variations of meteorological and other environmental conditions. Statistical analysis of the precursors goes beyond the scope of this paper, a probability study regarding a success rate of earthquake prediction and an alarm rate of earthquakes is now in progress, and will be reported in our succeeding paper. It is of high necessity currently to communicate rapidly the methods and results of the observation of precursors due to the frequent and future large earthquakes expected in Japan.

2 Method of High-Sensitivity Radiowave Observation

2.1 Geography of the Radiowave Observation

We observe radiowaves at three locations from different broadcast stations as shown in Fig. 1. The Iwata observation station (E137° 49'20", N34° 39'20", altitude 4m) is in Iwata city on the Pacific coastline, which receives two radiowaves: one at 79.2 MHz of power 1 kW, horizontal polarization from a broadcast station in Shizuoka city (E138° 27'56", N34° 58'27", alt. 300m), and the other at 78.9 MHz, 3 kW, horizontal polarization from a broadcast station in Tsu city (E136° 26'01", N34° 43'57", alt. 320m). The Toyama observation station (E137° 11'13", N36° 41'38", alt. 30m) is in Toyama city and placed on top of a building, which receives a radiowave at 82.3 MHz 1 kW, horizontal polarization from a broadcast station in Niigata city (E138° 48'30", N37° 42'24", alt. 600m), both on the west side of Japan. The Yatsuo observation station (E137° 07'51", N36° 37'10", alt. 30m) is not shown in Fig. 1 but locates in Yatsuo district of only 10 km south of Toyama observation station and receives the same radiowave at 82.3 MHz from Niigata; measurement at nearby stations helps to distinguish artificial noises in the observed data.

2.2 Noise Reduction by Super-Narrowband Notch Filter and Measurement System

The radiowave measurement system is composed of standard Yagi antennas of 5 elements in horizontal polarization and digital radio receivers AOR AR5001D and/or AR2300, which are controlled by PCs. The radiowave is measured every 10 seconds at Toyama and Yatsuo stations, and every 20 seconds at Iwata station. For the stable detection of the precursors of earthquakes, elaborate noise reduction is essential in the measurement system. Super-narrowband notch (band-rejection) filters are inserted between the antenna and the receiver to reduce unwanted radiowaves from nearby broadcast stations by more than 20 dB, typically from −50 dBm signal

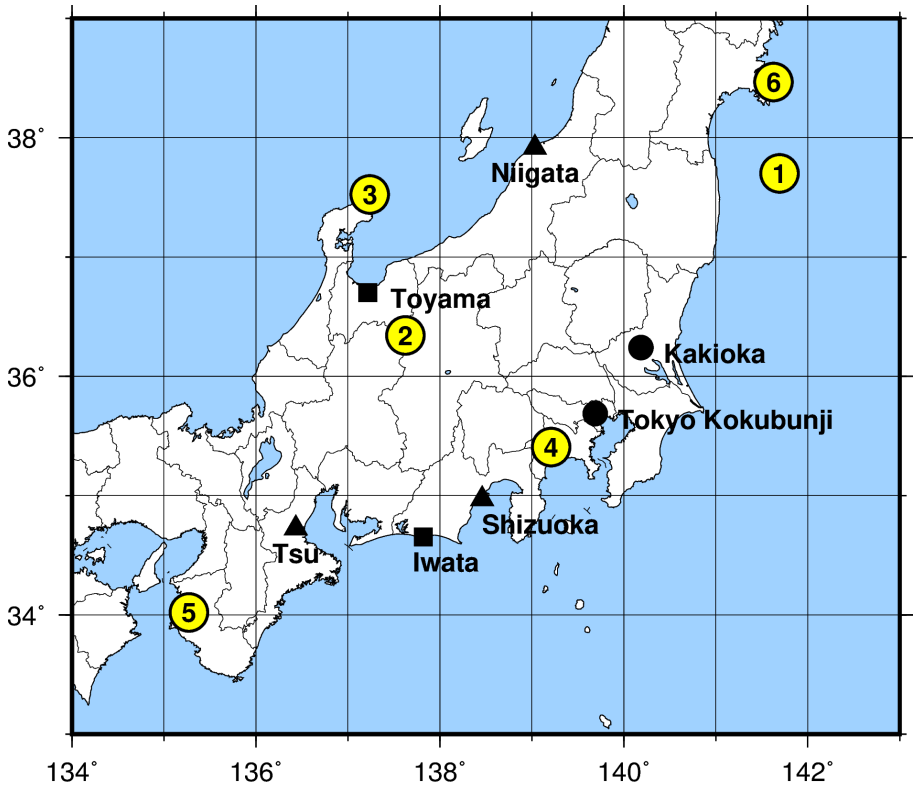

Figure 1. Locations of the radiowave broadcast stations (▲), radiowave observation stations (■), and meteorological observation facilities (●). Number inside a circle (○) denotes the approximate area of epicenters of the earthquakes of which shocks are detected near the radiowave observation station, i.e., 1: Fukushima offshore, 2: Gifu Hida district, 3: Ishikawa Noto district / Noto peninsula, 4: Kanagawa west, 5: Wakayama north / Kii channel, and 6: Miyagi offshore.

level down to −70 dBm, etc., which allows clear uninterrupted observation even in urban area.

The frequency characteristics of the super-narrowband notch filter used for the Toyama observation station is shown in Fig. 2 (a). The filter attenuates the radiowave signals from nearby stations each by −25 dB. Since the target signal from the Niigata broadcast station at 82.3 MHz is very close to the unwanted signal at 82.7 MHz, the target signal is also attenuated by approximately −11 dB; this may unfortunately degrades the necessary radiowave signal. However, the worse noise is the third-order intermodulation generated in the typical amplifying circuit of most of the receivers, which has been reduced by the filters by more than −30 dB, leading to the reduction of the noise floor under −90 to −100 dBm as shown in Fig. 2 (d). The effect of the filter is clearly seen when the filter is removed, e.g., for maintenance, on March 9th 12:00 to 17:00, the noise floor rose by 30 dB to 40 dB depending on the frequency. Reduction of the third-order intermodulation noise is thus found critical and given a higher priority than the slight loss of the necessary signal, otherwise, precursors are weak and hidden behind noises.

The super-narrowband notch filter is composed of a series capacitor of several pico-farad and a high-quality-factor (low-loss) inductance of approximately 1 nH. The inductance is realized by a short-circuited low-loss 12D-FB coaxial cable of length 60 cm to 70 cm, adjusted according to the frequency to be rejected, and has a quality-factor of approximately 25 to 30 at the VHF range. The circuit is shown in Fig. 2 (b) for a unit structure; for real use, a necessary number of the unit structures are cascaded as in Fig. 2 (c). We have thus achieved each rejection band as narrow as approximately 1 MHz, and the attenuation of more than 20 dB as in Fig. 2 (a). Note that usual commercial products of inductors are not applicable due to much larger loss or lower quality factor.

Similar notch filters are used for all the observation stations to attenuate unwanted radiowave signals and reduce the noise floor. There would be no need to go into a rural unpopulated district searching for a quiet environment if such filters are used in the observation system. In addition, coaxial cables connecting between antennas and receivers are loaded with numerous ferrite cores to reduce the common-mode noise. The target broadcast stations are chosen as many as possible in such a way that their radio signals are significantly weak but very close to the limit of detection. One needs to run the system for a certain period and seek for a radiowave that can carry anomalies under critical propagation conditions.

3 Observed Precursors of Earthquakes

Observed radiowave signals are shown in Figs. 3 to 6 together with other meteorological data: local precipitation, ionogram in Kokubunji (Tokyo), geomagnetic field in Kakioka, magnitude of the earthquake, Japan seismic intensity scale detected near the observation stations (local seismic intensity), and epicenters, all publicized officially by the Japan Meteorological Agency (JMA) and the National Institute of Communication Technologies (NICT), Japan. A radio signal at 80.9 MHz is monitored, where no broadcast signal exists in Japan; this helps to distinguish noises radiated from other wideband electromagnetic sources. Right above each plots, the broadcast stations from, and observation stations to which the radiowave is transmitted are shown, together with the frequency and the power of the radiowave. Notation '(H)' shows that the transmitting or receiving antenna is horizontally polarized. We also measure vertically polarized radiowaves, although not addressed in this paper but will be discussed in our succeeding paper.

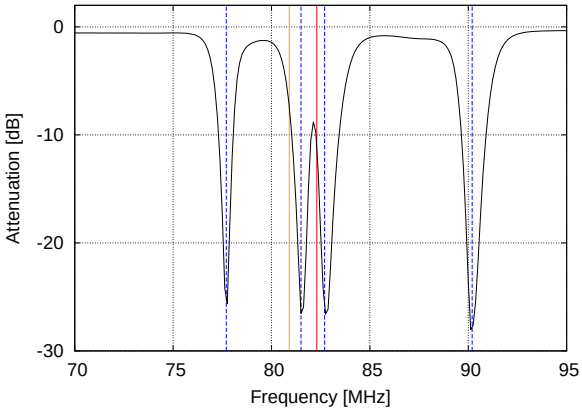

(a)

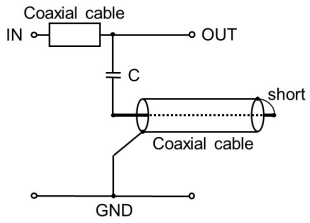

(b)

(c)

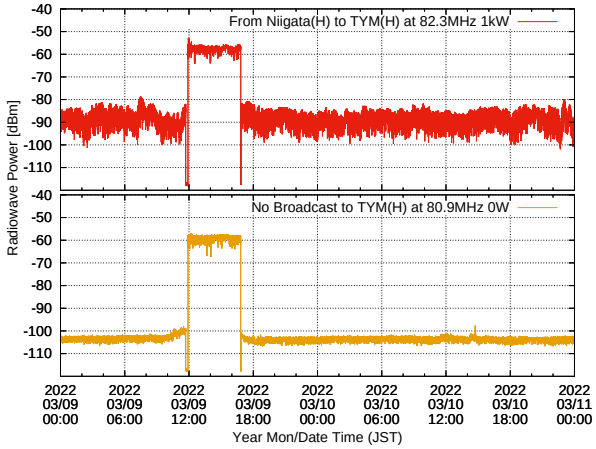

(d)

Figure 2. The super-narrowband notch filter implemented in the observation equipment. (a) Frequency characteristics of the whole filter. Blue dotted lines are the frequencies to be rejected i.e., 77.7 MHz, 81.5 MHz, 82.7 MHz and 90.2 MHz for the Toyama station, and the orange and the red solid lines are the target frequencies to be observed at 80.9 MHz and 82.3 MHz, respectively. (b) Unit circuit of the notch filter. (c) The appearance of the whole filter. Total 8 units are cascaded to reject 4 frequencies. The coaxial cables are rolled to fit in a 25 cm × 30 cm × 10 cm-high box. (d) Noise reduction effect of the filter; the filter was removed on March 9th 12:00 to 17:00 for maintenance, otherwise connected. The height of the step is the level of the noise reduction.

We have been detecting electromagnetic precursors of earthquakes steadily since the observation started about 5 years ago; remarkable ones among them are those associated with the earthquake of Fukushima offshore M7.4 on March 16, 2022, at 23:36:32.6 Japan Standard Time (JST), depth 57 km, maximum seismic intensity of Japan scale 6+. Since some days before the event, we have received precursory signals shown in Figs. 4 and 6. The local seismic intensity detected near the Iwata observation station was 4, and that near the Toyama observation station was 5−, as shown on top of Figs. 4 and 6.

Another earthquake had occurred one year before the Fukushima offshore M7.4 at the same location and depth, with the same level of magnitude, which is Miyagi offshore M6.9 on March 20, 2021, at 18:09:44.8 JST, depth 59 km, maximum seismic intensity 5+. The observed radiowave signal is shown in Figs. 3 and 5. For this event, the local seismic intensity observed near the Iwata observation station and the Toyama observation station was both 4 as shown on top of Figs. 3 and 5.

In Figs. 3 and 4, clear precursors of sudden rises and falls are seen over several hours, as highlighted by the yellow background, one to two days before the main shocks. The power level at 80.9 MHz stays the same for both cases, which indicates that the precursors are not of any other wideband noises. Moreover, changes in the weather and the ionograms are only marginal, thereby the precursors are not originated from the influence of the weather or the ionospheric layers. In Fig. 3, relatively large earthquakes occurred in Wakayama north (see area no. 5 in Fig. 1) on March 15, 2021, at 0:25:59.3 JST with M4.6 depth 4 km; small precursors are seen on March 12, 2021. Note that the variation of the signal on March 15, 2021, at around 1:00 to 4:00 JST in Fig. 3 is not an anomaly but an artificial noise where the radiowave is stopped temporarily for regular maintenance of the broadcast stations in Monday early morning. A small signal variation is again seen on March 16 in the same data only a few hours before Ibaraki south earthquake (not shown in Fig. 1 but Pacific side of Japan) on March 16, 2021, at 4:56:18.1 JST with M4.9 depth 54 km.

In Fig. 4, smaller signal variations are also seen in 78.9 MHz data, which could be due partly to the smaller earthquakes around March 11 to March 15, 2022 but may have been influenced in some degree from the crustal stress that caused the event of Fukushima offshore M7.4 on March 16. In Figs. 3 and 4, other data of precipitation, temperature, ionograms show no changes simultaneously with those of the radiowave signals, which show that there is only a minimal possibility that the changes in the radiowave signals are caused by the meteorological or ionospheric conditions. The geomagnetic field show some ripples on March 20, 2021, as shown in Fig. 3, which might have some relation to the earthquake on the same day. However, the electromagnetic precursors do not coincide with the geomagnetic field ripples. Moreover, as in Fig. 4, notable changes are not seen in the geomagnetic field synchronously either with the precursors or with the main shock.

In Figs. 5 and 6, precursors are also seen, at Toyama and Yatsuo observation stations on the west side of Japan, as highlighted by yellow backgrounds, before the large earthquakes of Miyagi offshore M6.9 and Fukushima offshore M7.4. The time variation of the radiowave power behaves similarly to those of Iwata as in Figs. 3 and 4. Smaller earthquakes occurred in Ishikawa Noto, Gifu Hida (see area no. 3 and 2, respectively, in Fig. 1) and so on for both cases before the large events in Miyagi and in Fukushima, and smaller precursory signals are also seen slightly before the smaller earthquakes. And approximately one day before the main shocks, the largest variations in the time signal are seen as highlighted by yellow in Figs. 5 and 6; these are considered as precursors of the main earthquakes. In those figures, there is no obvious evidence that the meteorological, ionospheric, and geomagnetic field conditions generated the precursory signals, which is also the case for the precursors that we have detected so far.

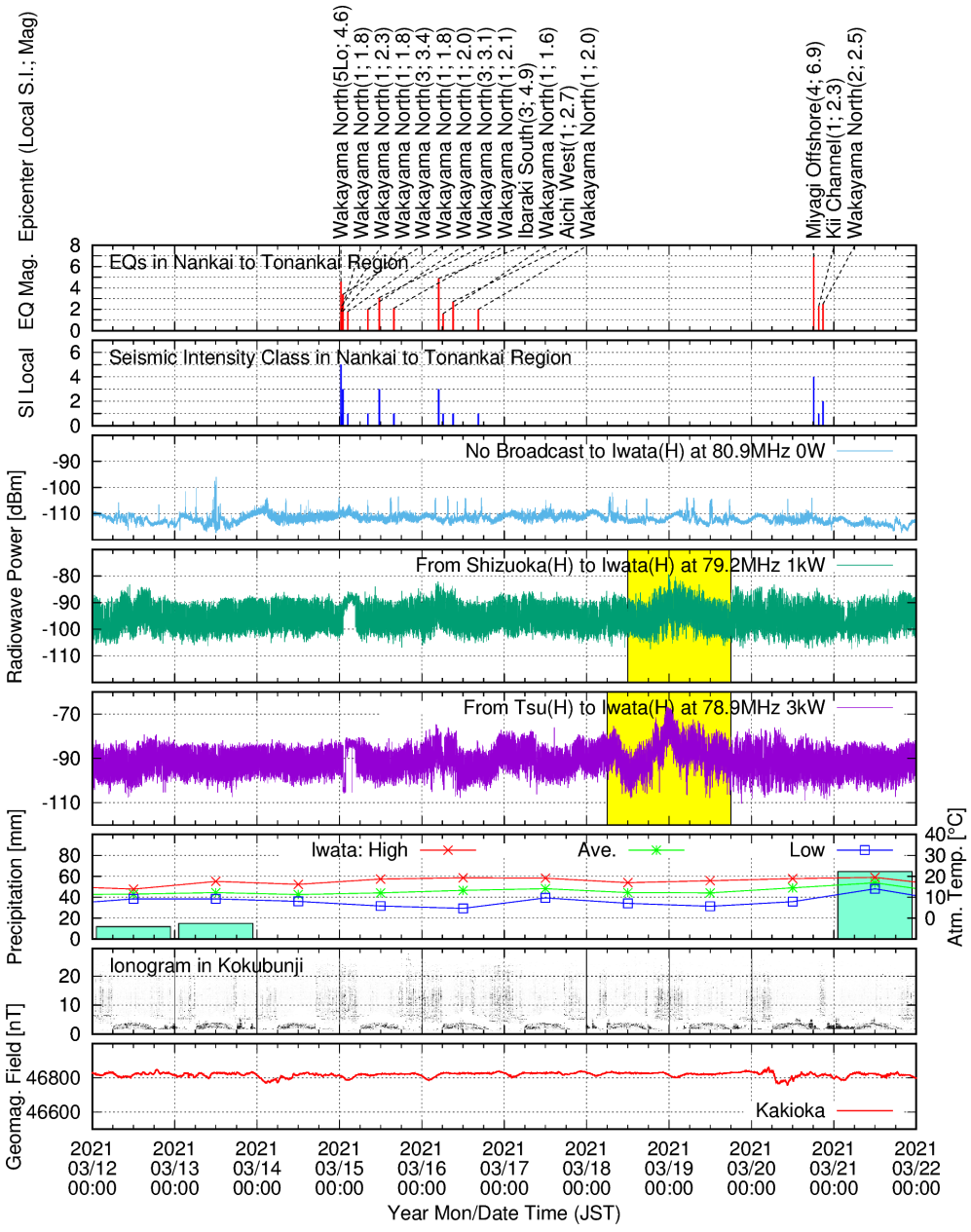

Figure 3. Observed radiowave power (dBm) at Iwata observation station on the Pacific side of Japan in March 2021, together with environmental data observed by national institutes.

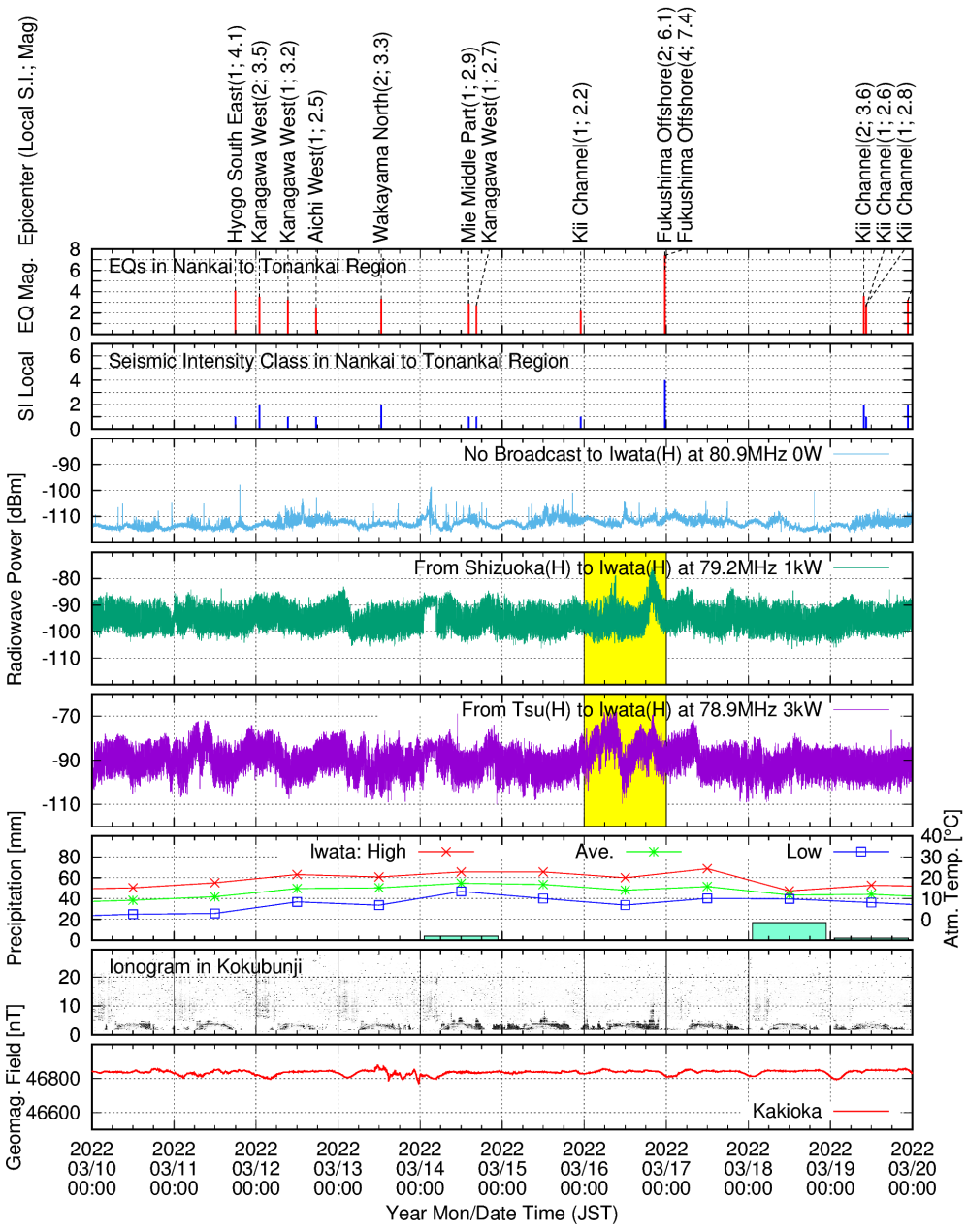

Figure 4. Observed radiowave power (dBm) at Iwata observation station on the Pacific side of Japan in March 2022, together with environmental data observed by national institutes.

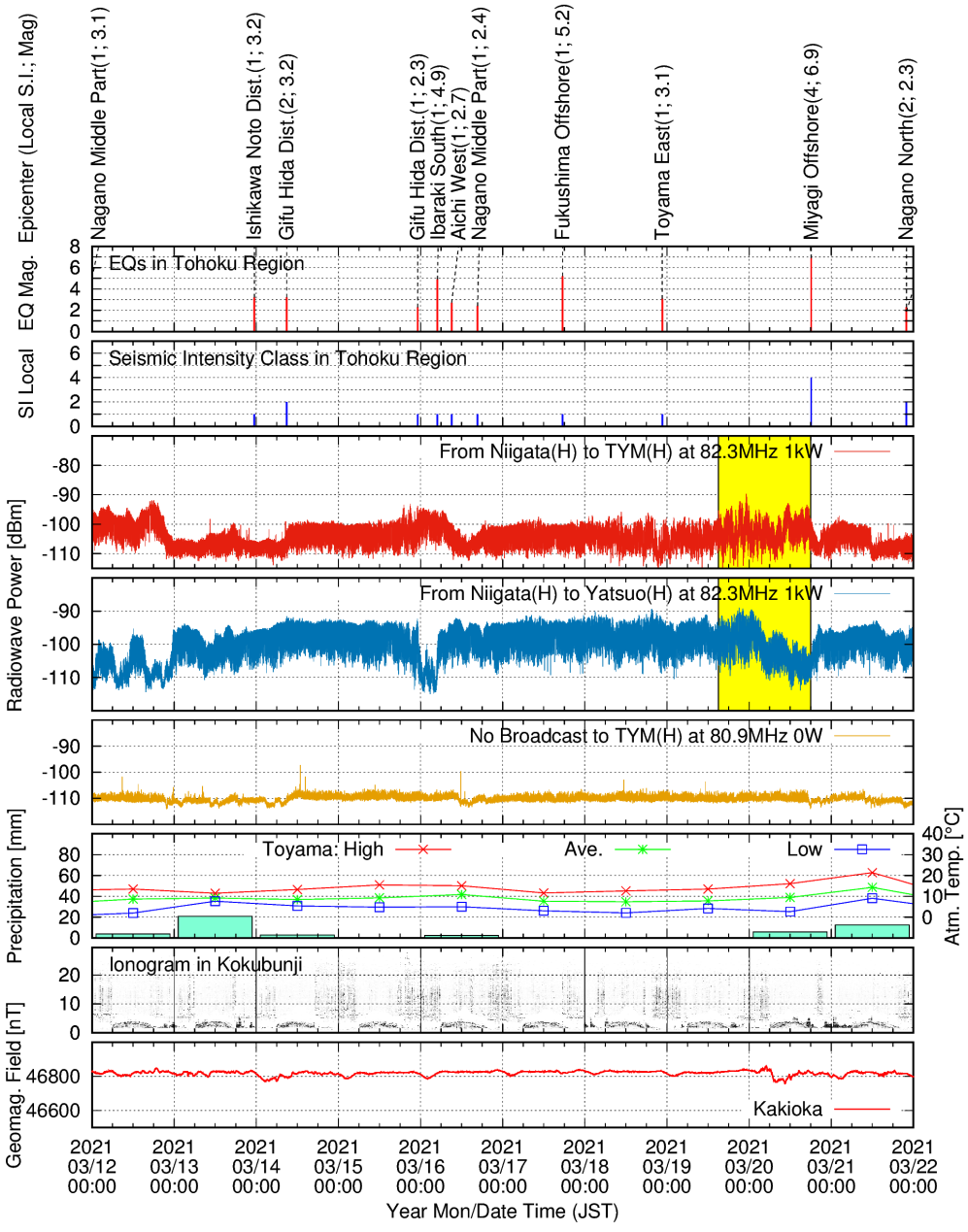

Figure 5. Observed radiowave power (dBm) at Toyama (TYM) and Yatsuo observation stations on the west side of Japan in March 2021, together with environmental data observed by national institutes.

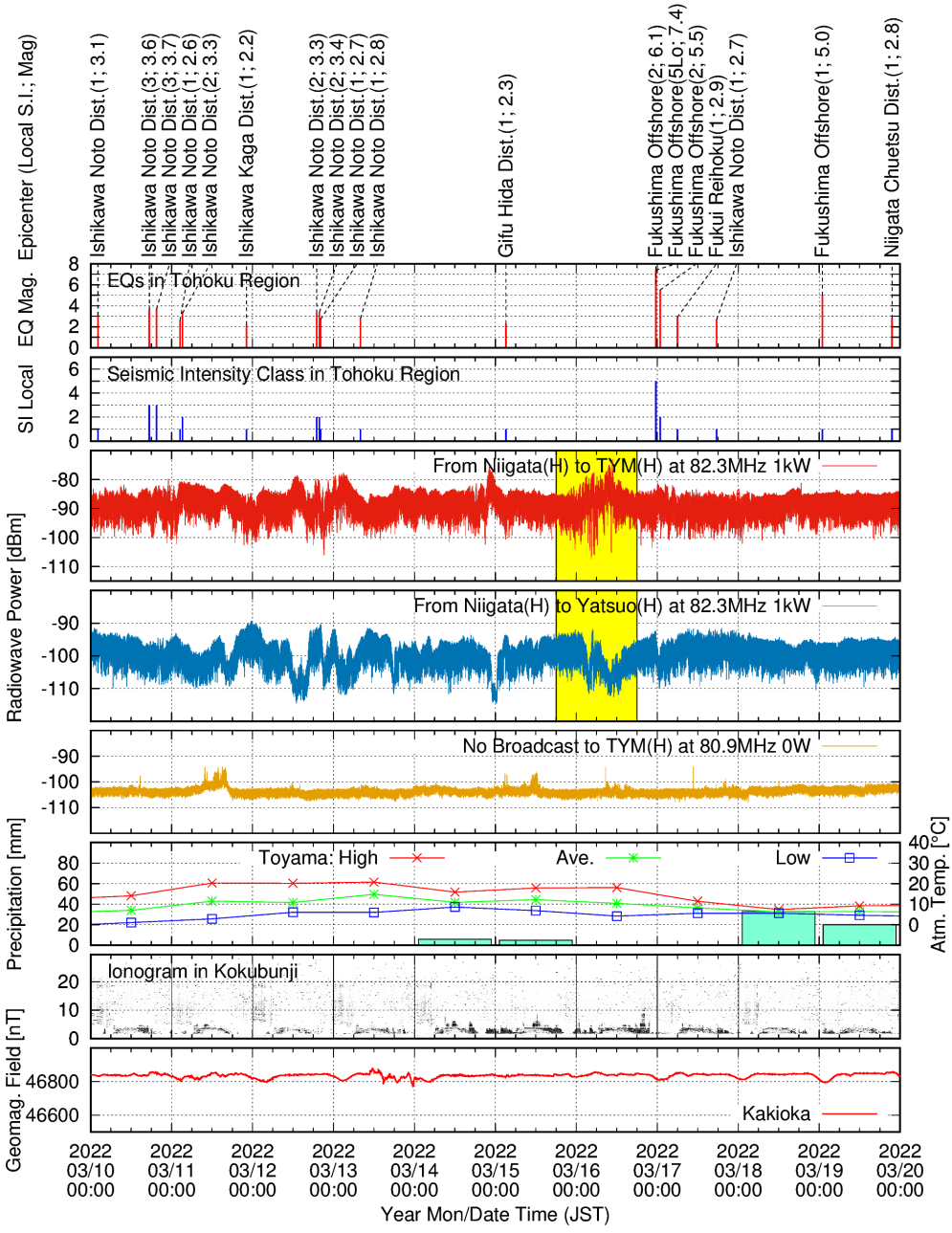

Figure 6. Observed radiowave power (dBm) at Toyama (TYM) and Yatsuo observation stations on the west side of Japan in March 2022, together with environmental data observed by national institutes.

It is also interesting to note in Figs. 5 and 6 that the variations of the radiowave power observed in Toyama (TYM) and those in Yatsuo are mostly opposite regarding its increase or decrease; these observation stations are as short a distance as 10 km apart, for which an opposite behavior of the received power cannot be explained by the simple meteorological radio ducting or any other influence from ionospheric layers. When the radiowave power is stronger in Toyama, it is weaker in Yatsuo, which implies that the radiowave, radiated from Niigata, is focused slightly northward to the direction toward Toyama than toward Yatsuo. Such beam-steering-like propagation of a radiowave is explained by the random but steep focusing effect of the terrestrial surface plasmon on mountain ranges, which can depend on the geography, induced plasma frequency, and thus the strength of the seismic activity (Fujii, 2014, 2016). The observation station in Toyama (TYM) is on the west side of Japan island, more than 300 km away from the epicenters on the Pacific side. The crustal structure in this district is complicated and consists of intricate large faults. Considering those facts and possible mechanisms that relate to the propagation of charges through lithospheric structures and faults, it is inferred that the precursors may travel over a long distance to reach the other side of the island.

It is worth noting that the precursors in Figs. 3 to 6 have similarity and simultaneity, despite that the observation stations are more than 200 km apart; those precursors are plotted together and compared in detail in Figs. 7 and 8. Note the time of the two observation systems are synchronized by the internet time server, and the time difference is less than a second. The simultaneity of the precursors for Miyagi offshore M6.9 in Fig. 7 between Toyama (TYM) 82.3 MHz and Iwata 78.9 MHz are slightly weaker than the case for Fukushima offshore M7.4 in Fig. 8 (a); this could be due to the fact that the Magnitude is smaller, and the epicenter is more distant.

On the other hand, in Fig. 8 (a), the precursors appear simultaneously in the morning of March 16, 2022, in Toyama (TYM) 82.3 MHz and in Iwata 78.9 MHz data. Intense oscillations (with yellow highlight) are observed with a time scale of 1 to 2 hours. Those are typical precursors so far observed before large earthquakes. More detail of the signal exhibits some differences as shown in Fig. 8 (b) on the day of the earthquake between the signal in Toyama (TYM) 82.3 MHz and that in Iwata 78.9 MHz; i.e., some sudden drops are seen in Toyama (TYM) 82.3 MHz, while they are not seen in Iwata 78.9 MHz. If the radiowave anomalies occur solely in the atmosphere near the epicenter, they must appear simultaneously and identically because the radiowave propagates at the speed of light. The difference of the anomaly could be the evidence that the anomaly occurs not only in the atmosphere but is mediated by some other mechanisms such as those on the ground surface and/or underground.

Electromagnetic precursors are now detected reliably and steadily, at least near the area of observation of the radiowave propagation, which tells us chronological information about the impending earthquakes, i.e., it tells if an earthquake is ready to occur shortly or not. The information on the location of the lithospheric stress and seismic activity would be obtained by placing more observation stations and considering the radiowaves paths that may carry such precursors, as well as accumulating the data of precursors and earthquakes that happened.

4 Conclusions

It has been shown that clear electromagnetic precursors are detected in VHF radiowave signals before Fukushima offshore M7.4 earthquake on March 16, 2022, by using high-sensitivity low-noise observation systems employing super-narrowband notch filters. Precursors are detected consistently and steadily with the proposed observation systems. We have detected similar precursors at two distant locations for the large earthquake, which are considered to be the evidence of the precursors.

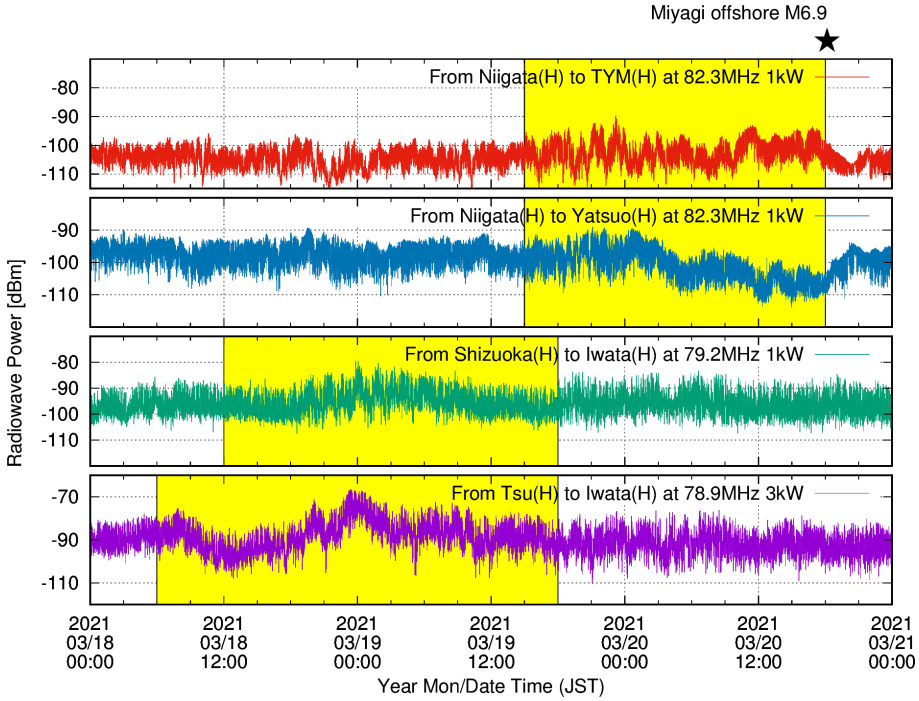

Figure 7. Expansion and comparison of the precursory signals observed in Iwata, Toyama and Yatsuo for March 2021. Star symbol shows the time of the earthquake. Yellow-highlighted periods are the same as in Figs. 3 and 5.

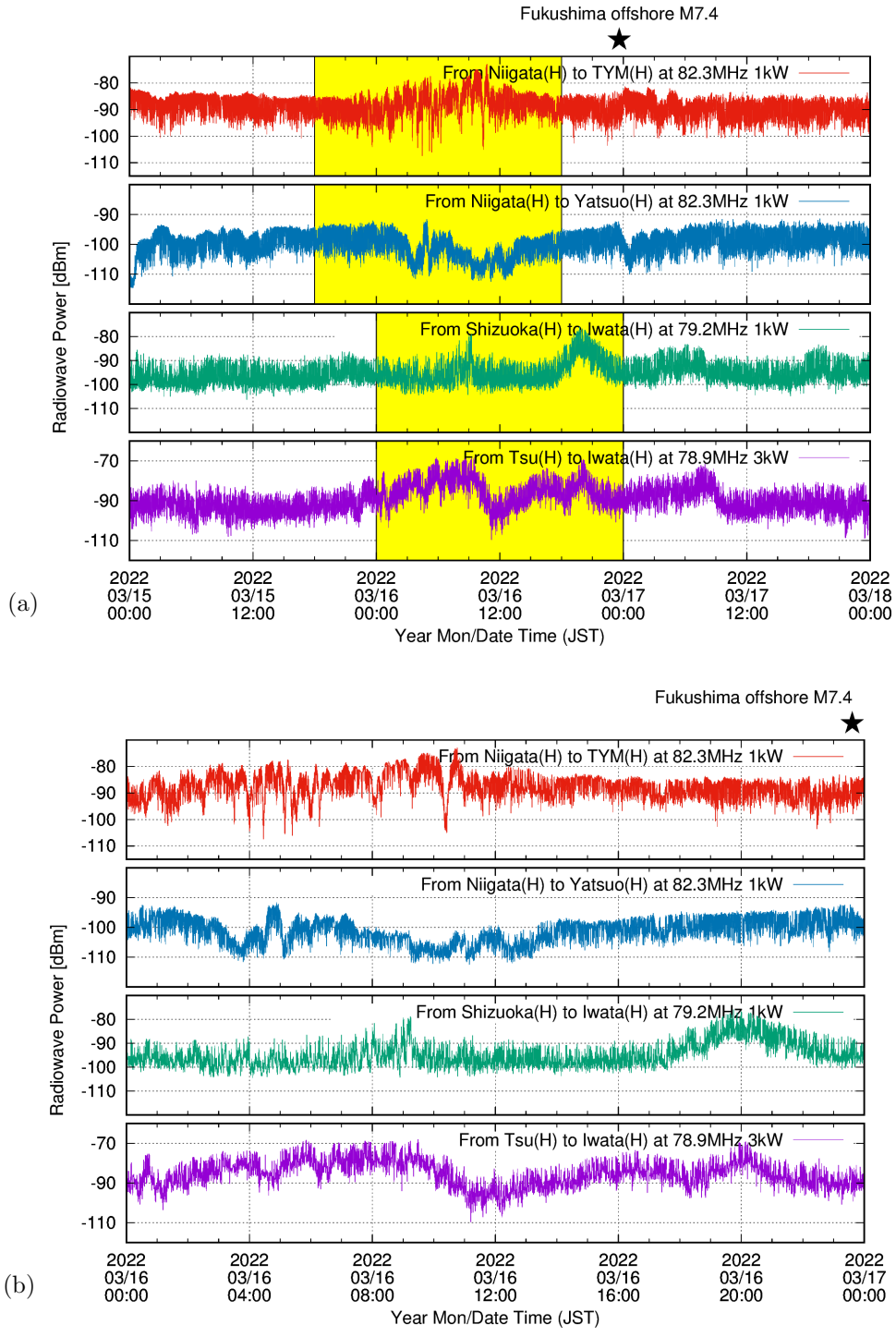

Figure 8. Expansion and comparison of the precursory signals observed in Iwata, Toyama and Yatsuo for March 2022. Star symbol shows the time of the earthquake. (a) Comparison of data for 3 days around the day of the earthquake. Yellow highlighted periods are the same as in Figs. 4 and 6. (b) More detail on the day of the earthquake.

More detailed results and statistical analyses of the observation will be reported in our succeeding paper. Although the epicenter of earthquakes has not been predicted accurately yet, by placing more observation stations and accumulate the data of precursors and succeeding earthquakes, reliable prediction of large earthquakes will certainly be possible, which has long been a dream of human beings.

5 Open Research

Data of earthquakes from the searching service by the Japan Meteorological Agency (JMA) available at `https://www.data.jma.go.jp/svd/eqdb/data/shindo/index.html` (*Japan Meteorological Agency Seismic Intensity Database Search*, n.d.). Precipitation and Temperature data from JMA at `https://www.data.jma.go.jp/obd/stats/etrn/` (*Japan Meteorological Agency Previous Weather Data Search*, n.d.). Ionograms from the National Institute of Communication Technologies (NICT), Japan at `https://wdc.nict.go.jp/cgi-bin/ionog/sum_control.cgi` (*Ionosheric Sounding Data in Japan, Ionogram*, n.d.). Geomagnetic field data from JMA Kakioka Magnetic Observatory at `http://www.kakioka-jma.go.jp/obsdata/metadata` (*Geomagnetic Digital Data Service*, n.d.).

Radiowave data and other environmental data integrated into synchronized diagrams by the author available at `http://www3.u-toyama.ac.jp/densou01/RadiowaveDataPlots_5.5c_nohighlight/RadiowaveDataPlots_Shizuoka_Iwata_all.pdf` and `http://www3.u-toyama.ac.jp/densou01/RadiowaveDataPlots_5.5c_nohighlight/RadiowaveDataPlots_Toyama_Toyama_all.pdf`.

Figures were made with Gnuplot version 5.2.8 available under Copyright by T. Williams, and C. Kelley at `http://www.gnuplot.info` (Williams & Kelley, n.d.).

Map was created using Generic Mapping Tools (GMT) version 5.4.5, under Copyright by The GMT Developers (2019 - 2022) available at `https://www.generic-mapping-tools.org` (Wessel, n.d.).

Acknowledgments

This work is partly supported by the Japan Society for the Promotion of Science (JSPS) KAKENHI Grant Number 21K04059.

References

Bakun, W. H., Aagaard, B., Dost, B., Ellsworth, W. L., Hardebeck, J. L., Harris, R. A., ... Lienkaemper, J. J. (2005, Oct.). Implications for prediction and hazard assessment from the 2004 Parkfield earthquake. *Nature*, *437*(13), 969-974.

Bleier, T., Dunson, C., Roth, S., Heraud, J., Lira, A., Freund, F., ... Papadopoulos, G. (2013). Earthquake prediction studies: Seismo electromagnetics. In (p. 1-15). Terrapub. (Edited by M. Hayakawa)

Freund, F. (2000). Time-resolved study of charge generation and propagation in igneous rocks. *J. Geophysical Res., Solid Earth*, *105*(B5), 11001-11019.

Freund, F. (2002). Charge generation and propagation in igneous rocks. *J. of Geodynamics*, *33*, 543-570.

Freund, F. (2011). Pre-earthquake signals: underlying physical processes. *J. of Asian Earth Sciences*, *41*, 383-400.

Fujii, M. (2013, Mar.). Theory of ground surface plasma wave associated with pre-earthquake electrical charges. *Radio Science*, *48*, 122-130.

Fujii, M. (2014, Mar.). Fundamental correction of Mie's scattering theory for the analysis of plasmonic resonance of a metal nanosphere. *Phys. Rev. A*, *89*(3), 033805.

Fujii, M. (2016, Aug.). A new mode of radio wave diffraction via the terrestrial surface plasmon on mountain range. *Radio Science*, *51*, 1396-1412.

Fujiwara, H., Kamogawa, M., Ikeda, M., Liu, J. Y., Sakata, H., Chen, Y. I., ... Ohtsuki, Y. H. (2004). Atmospheric anomalies observed during earthquake occurrences. *Geophys. Res. Lett.*, *31*, L17110.

Geomagnetic digital data service [Dataset]. (n.d.). Japan Meteorological Agency Kakioka Magnetic Observatory. Retrieved from `http://www.kakioka-jma.go.jp/obsdata/metadata`

Hayakawa, M., Surkov, V. V., Fukumoto, Y., & Yonaiguchi, N. (2007). Characteristics of VHF over-horizon signals possibly related to impending earthquakes and a mechanism of seismo-atmospheric perturbations. *J. of Atmospheric and Solar-Terrestrial Phys.*, *69*, 1057-1062.

Ionosheric sounding data in japan, ionogram [Dataset]. (n.d.). National Institute of Communication Technologies. Retrieved from `https://wdc.nict.go.jp/cgi-bin/ionog/sum_control.cgi`

Japan meteorological agency previous weather data search [Dataset]. (n.d.). Japan Meteorological Agency. Retrieved from `https://www.data.jma.go.jp/obd/stats/etrn/`

Japan meteorological agency seismic intensity database search [Dataset]. (n.d.). Japan Meteorological Agency. Retrieved from `https://www.data.jma.go.jp/svd/eqdb/data/shindo/index.html`

Kittel, C. (1986). *Introduction to solid state physics* (6th ed.). New York: John Wiley and Sons, Inc.

Kushida, Y. (2012). *Earthquake forcast.* Tokyo: PHP Shinsho. (in Japanese)

Moriya, T., Mogi, T., & Takada, M. (2010). Anomalous pre-seismic transmission of VHF-band radio waves resulting from large earthquakes, and its statistical relationship to magnitude of impending earthquakes. *Geophysical J. Int.*, *180*, 858-870.

Moriya, T., Mogi, T., Takada, M., & Kasahara, M. (2005, Mar.). Observational research for VHF (FM radio broadcasting waves) scattering waves as a precursor of earthquake occurrence. *Geophysical Bulletin of Hokkaido University*(68), 161-178. (in Japanese)

Moriya, T., Mogi, T., Takada, M., & Yamamoto, I. (2009, Mar.). Observational research for VHF scattering waves prior to earthquakes (II). *Geophysical Bulletin of Hokkaido University*(72), 269-285. (in Japanese)

Raether, H. (1977). Surface plasma oscillations and their applications. In (Vol. 9, p. 145-261). New York: Academic Press.

Raether, H. (1988). *Surface plasmons on smooth and rough surfaces and on gratings.* Berlin: Springer-Verlag. (p.5)

Scoville, J., Sornette, J., & Freund, F. (2015, Dec.). Paradox of peroxy defects and positive holes in rocks Part II: Outflow of electric currents from stressed rocks. *J. of Asian Earth Sciences*, *114-2*, 338-351.

Uyeda, S., Nagao, T., & Kamogawa, M. (2009). Short-term earthquake prediction: current status of seismo-electromagnetics. *Tectonophysics*, *470*, 205-213.

Wessel, P. (n.d.). *The generic mapping tools* [Software]. The GMT Developers. Retrieved from `https://www.generic-mapping-tools.org`

Williams, T., & Kelley, C. (n.d.). *Gnuplot homepage* [Software]. Retrieved from `http://www.gnuplot.info`